

The Unusual Rheology of Wormlike Micelles in Glycerol: Comparable Timescales for Chain Reptation and Segmental Relaxation

Niti R. Agrawal, Xiu Yue, and Srinivasa R. Raghavan*



Cite This: *Langmuir* 2020, 36, 6370–6377



Read Online

ACCESS |



Metrics & More

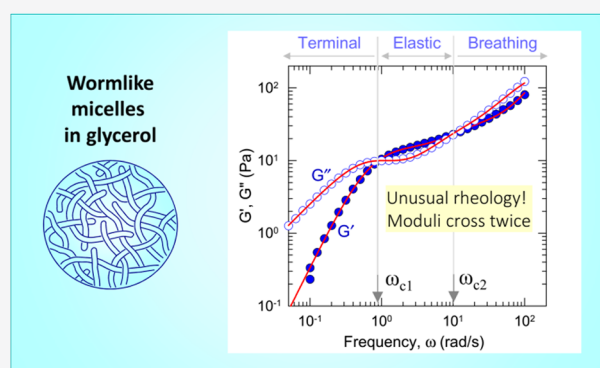


Article Recommendations



Supporting Information

ABSTRACT: Wormlike micelles (WLMs) are polymer-like chains formed by surfactant self-assembly in water. Recently, we have shown that WLMs can also be self-assembled in polar organic liquids like glycerol using a cationic surfactant and an aromatic salt. In this work, we focus on the dynamic rheology of the WLMs in glycerol and demonstrate that their rheology is very different from that of WLMs in water. Aqueous WLMs that are entangled into transient networks exhibit the rheology of a perfect Maxwell fluid having a single relaxation time t_R —thereby, their elastic modulus G' and viscous modulus G'' intersect at a crossover frequency $\omega_c = 1/t_R$. WLMs in glycerol also form entangled networks, but they are not Maxwell fluids; instead, they exhibit a double-crossover of G' and G'' (at ω_{c1} and ω_{c2}) within the ω -window accessible by rheometry (10^{-2} to 10^2 rad/s). The first crossover at ω_{c1} (~ 1 rad/s) corresponds to the terminal relaxation time (i.e., the timescale for chains to disentangle from the transient network and relax by reptation). At the other extreme, at frequencies above ω_{c2} (which is ~ 10 rad/s), the rheology is dominated by the segmental motion of the chains. This “breathing regime” has rarely been accessed via experiments for aqueous WLMs because it falls around 10^5 rad/s. We believe that glycerol, a solvent that is much more viscous than water, exerts a crucial influence in pushing ω_{c2} to 1000-fold lower frequencies. On the basis of the rheology, we also hypothesize that WLMs in glycerol are shorter and weakly entangled compared to WLMs in water. Moreover, we suggest that WLMs in glycerol are “unbreakable” chains—i.e., the chains remain mostly intact instead of breaking and re-forming frequently—and this polymer-like behavior explains why the samples are quite unlike Maxwell fluids.



INTRODUCTION

Wormlike micelles (WLMs) are long, flexible cylindrical chains formed by the self-assembly of surfactants.^{1–4} They share many similarities with polymers in solution,⁵ including the ability to entangle and form transient networks, which makes the solution highly viscous and viscoelastic. Most studies on WLMs have been conducted in water, and a typical formulation of aqueous WLMs consists of a cationic surfactant with a long tail (C_{16} or higher) combined with a salt.^{1–4} Typical surfactants include cetylpyridinium chloride (CPyCl) or cetyltrimethylammonium bromide (CTAB). The salt can be either a simple one like sodium perchlorate (NaClO_3) or one with an aromatic counterion that binds to the micelles like sodium salicylate (NaSal). WLMs in water tend to have diameters around 5 nm (the diameter is about twice the length of the surfactant tail) and contour (end-to-end) lengths L ranging from 100 to 5000 nm.^{3,5} This in turn implies that their aggregation numbers N_{agg} (i.e., the number of molecules associated into a micelle) are ~ 1000 or higher, on average.

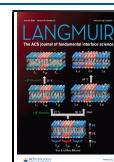
In a recent study, we have demonstrated that WLMs can be formed in polar organic solvents such as glycerol and

formamide.⁶ To our knowledge, this is the first report of WLMs in pure solvents of intermediate polarity. Previous studies in these solvents had only reported small micelles with N_{agg} of 100 or lower.^{7,8} The system we studied contained a cationic surfactant with a long (C_{22}) tail, erucyl bis-(hydroxyethyl)methylammonium chloride (EHAC), along with the aromatic salt, NaSal. Equimolar mixtures of EHAC and NaSal gave rise to WLMs in glycerol, and the resulting samples were viscoelastic and flow-birefringent, much like aqueous WLMs.⁶ Interestingly, while simple salts like NaCl are known to induce WLMs of EHAC in water,⁹ this was not the case in glycerol—only binding salts like NaSal induced WLMs in the latter case. We also formed EHAC–NaSal WLMs in a 90–10 solvent mixture of glycerol and ethylene glycol, which

Received: February 21, 2020

Revised: May 19, 2020

Published: June 3, 2020



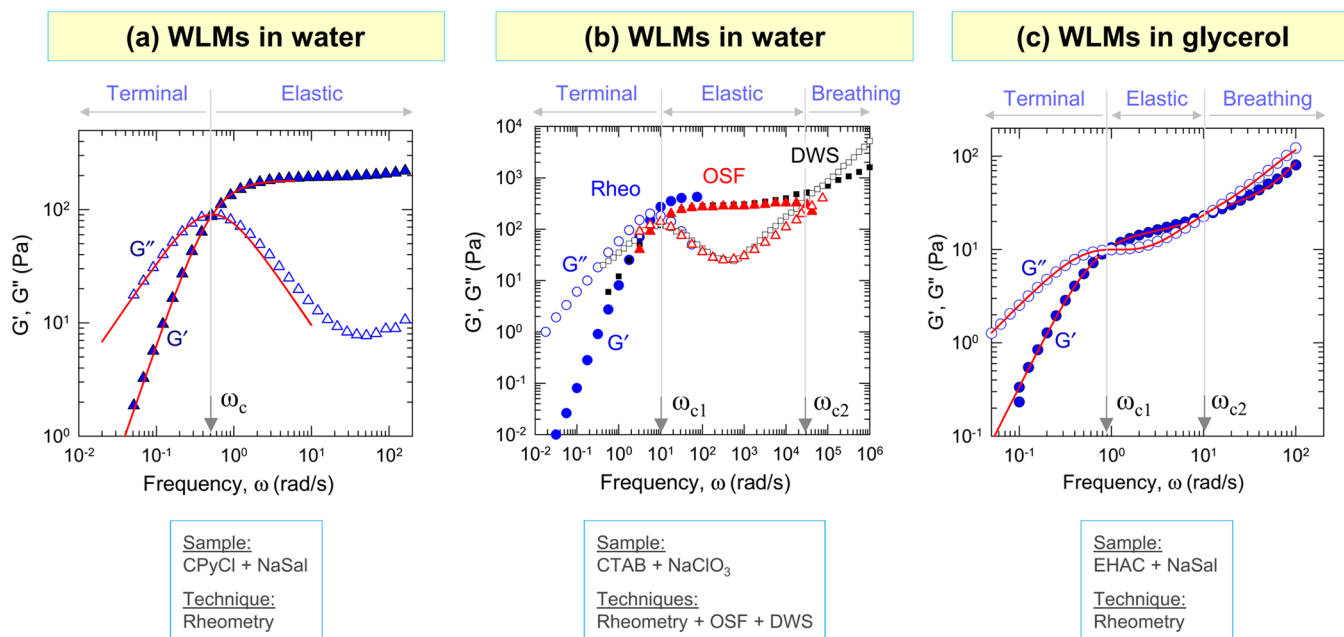


Figure 1. Comparing the dynamic rheology of WLMs in water and glycerol. In all cases, the elastic modulus G' and the viscous modulus G'' are plotted vs frequency ω . (a) Typical WLMs in water (235 mM CPyCl + 125 mM NaSal) show the rheology of a single- t_R Maxwell fluid (lines are fits to this model). The data are from rheometry at 22 °C.¹³ (b) Data for WLMs of 60 mM CTAB + 100 mM NaClO₃ in water are shown over a wider range of ω by combining measurements from rheometry, oscillatory squeeze flow (OSF) and diffusive wave spectroscopy (DWS), all at 30 °C.¹⁴ In this case, G' and G'' cross twice (at ω_{c1} and ω_{c2}), and thereby the data are demarcated into three regimes. (c) Typical WLMs in glycerol (60 mM EHAC + 60 mM NaSal) show two crossovers of the moduli as in (b), but over a much narrower range of ω . The data are entirely from rheometry at 25 °C. Lines are fits to a 3-mode Maxwell model.

had a freezing point well below 0 °C.⁶ Thereby, we were able to confirm the existence of WLMs at subzero temperatures in these systems.

In this work, we focus on the rheology of WLMs in glycerol. In our previous paper, we had briefly presented the dynamic rheology, i.e., plots of the elastic modulus (G') and viscous modulus (G'') against frequency ω , for one of those samples.⁶ The data exhibited several unusual features that made it distinct from the rheology of WLMs in water. From a rheological perspective, WLMs (in water) are considered a model viscoelastic fluid because their dynamic rheology (in the regime where the chains are entangled into a network) closely follows the Maxwell model of viscoelasticity with a single relaxation time t_R .^{1,3} For such a Maxwell fluid, G' and G'' will show a single crossover at a frequency ω_c from which $t_R = 1/\omega_c$ can be estimated.^{10,11} In contrast, we find that WLMs in glycerol exhibit not one, but two, crossovers of G' and G'' —at frequencies of ω_{c1} and ω_{c2} . Thus, the dynamic frequency spectrum of these WLMs is quite unusual and can be demarcated into three regimes. Here, we discuss this rheological pattern in detail and document the differences in rheology between WLMs in glycerol and water. We will then attempt to explain *why* the differences arise, i.e., to elucidate the unique attributes of WLMs in glycerol and other polar solvents.

EXPERIMENTAL SECTION

Materials. The surfactant erucyl bis(hydroxyethyl)-methylammonium chloride (EHAC) was obtained from Akzo Nobel. EHAC was dried in a vacuum oven at room temperature before use. Sodium salicylate (NaSal) and glycerol (Gly) were obtained from Sigma-Aldrich.

Sample Preparation. Stock solutions of EHAC and NaSal were prepared by adding weighed amounts of each into glycerol and

heating to ~ 60 °C on a hot plate under constant stirring for 4–5 h. After clear solutions were obtained, they were cooled and stored at room temperature. Both EHAC and NaSal are completely soluble in glycerol over the concentration range studied in this work. To prepare a sample with desired molar concentrations of surfactant and salt, the respective stock solutions were combined and diluted with the solvent. After vortex mixing, the sample was heated to 60 °C for 10–15 min and then cooled to room temperature. Samples were left at room temperature for at least a day before any measurements.

Rheology. Rheological experiments were conducted on an AR2000 stress-controlled rheometer (TA Instruments). A cone-and-plate geometry (2° stainless steel cone, 20 mm diameter) was used to perform the experiments. The temperature was controlled by a Peltier assembly on the rheometer, which employed a circulating fluid fed from a chiller. Rheological experiments were conducted at temperatures ranging from 10 to 50 °C. Dynamic frequency sweep experiments were conducted in the linear viscoelastic regime for each sample, which was determined from strain-sweep experiments. The frequency range for these experiments was typically between 0.1 to 100 rad/s. Frequencies above 100 rad/s were not explored because inertial effects in the rheometer can potentially distort the data.

RESULTS AND DISCUSSION

Typical Rheology of WLMs in Water and Glycerol.

WLMs in water are known to be single- t_R Maxwell fluids, even though the chains are highly polydisperse in their length. The reason for this behavior was explained by Cates in the late 1980s.^{1,12} WLMs can release an applied stress in two ways. First, the chains can relax by reptation, much like polymers, and this is associated with a reptation time t_{rep} . However, unlike polymers, WLM chains can also undergo reversible scission, i.e., they can break into segments, or broken segments can recombine into a whole. Micellar breaking provides a second mode for stress-relaxation in the case of WLMs that is absent for polymers, and this is associated with a breaking time

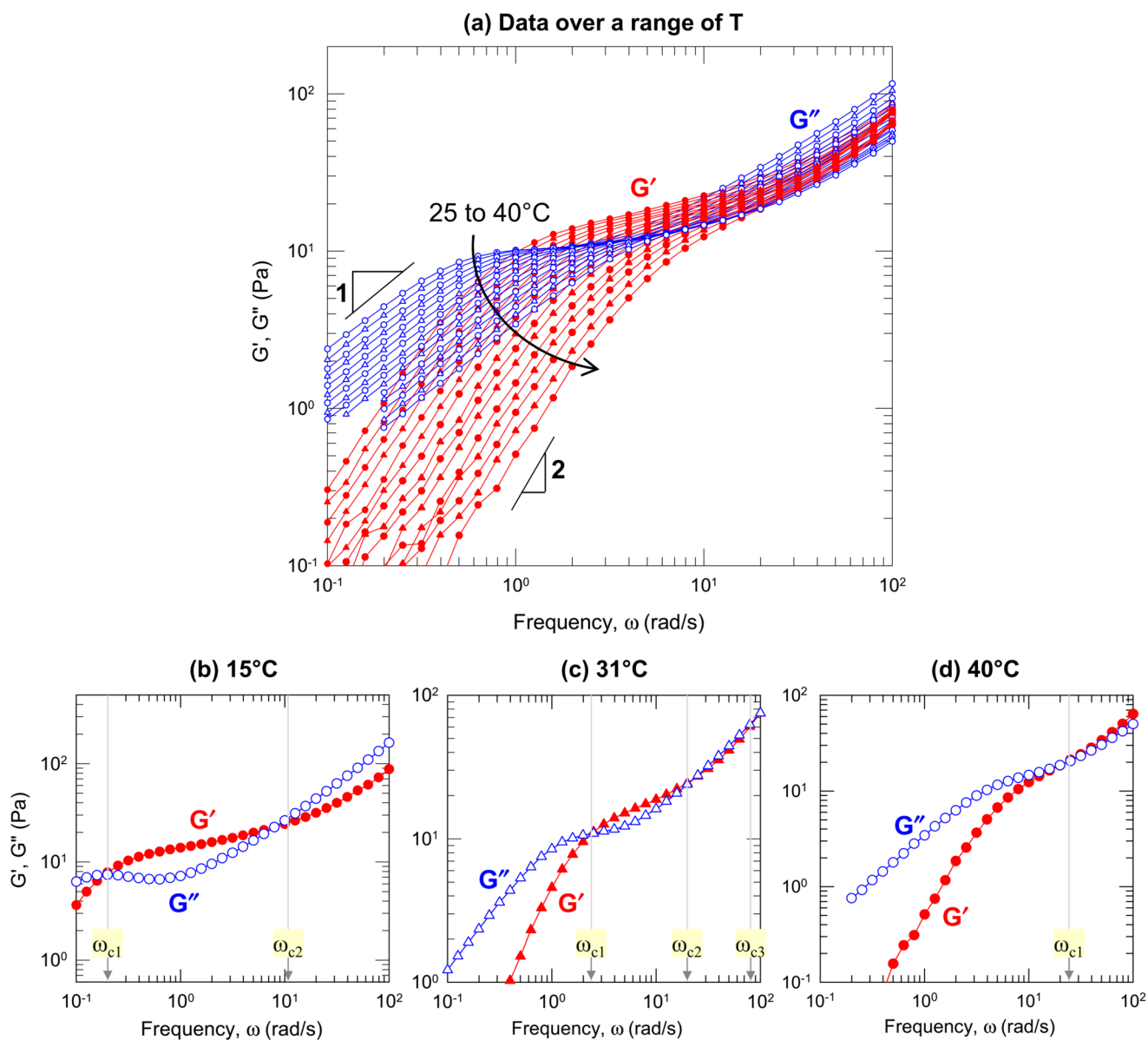


Figure 2. Dynamic rheology of WLMs in glycerol over a range of temperatures. The sample consists of 60 mM EHAC + 60 mM NaSal. (a) Data over a temperature range from 25 to 40 °C. The elastic modulus G' and the viscous modulus G'' are plotted vs frequency ω at each temperature. (b–d) The moduli at specific temperatures are shown to indicate distinct patterns in the data.

t_{br} . Cates predicted that, for the case of “fast-breaking” WLMs with $t_{br} \ll t_{rep}$, the rheology would be that of a Maxwell fluid,^{2,12} and that the single relaxation time $t_R = (t_{br} \cdot t_{rep})^{0.5}$. Indeed, many WLM samples in water behave like Maxwell fluids, and an example is shown in Figure 1a.¹³ The sample consists of the cationic surfactant cetylpyridinium chloride (CPyCl, 235 mM) combined with 125 mM NaSal in water at 22 °C. The data, which are from an earlier paper from our lab,¹³ were obtained using rheometry. Plots of G' and G'' vs frequency ω are shown, and the lines through the data are fits to a single- t_R Maxwell model as per the equations:^{10,11}

$$G'(\omega) = \frac{G_p \omega^2 t_R^2}{1 + \omega^2 t_R^2}; \quad G''(\omega) = \frac{G_p \omega t_R}{1 + \omega^2 t_R^2} \quad (1)$$

where G_p is the plateau modulus, i.e., the value of G' at high ω . Note that G' and G'' intersect once at the crossover frequency

$\omega_c = 0.46$ rad/s, from which $t_R = 1/\omega_c$ can be estimated to be 2.2 s.

The data in Figure 1a are demarcated into two distinct regimes based on ω .^{10,11} The region for $\omega < \omega_c$ is the “terminal” regime where $G'' > G'$, indicating viscous behavior, with the slopes of the moduli being 1 and 2 on the log–log plot. In this regime, the timescales are long enough for the WLMs to disengage from their transient network and relax slowly.^{1,12} At shorter timescales, i.e., for $\omega > \omega_c$, there is the “elastic” regime, where G' plateaus at G_p and $G' > G''$.^{10,11} At these timescales, the rheology reflects the intact network of WLMs connected by entanglements.^{1,12} Midway through this elastic regime, G'' reaches a minimum and then begins an upturn at higher ω . However, a second crossover of G'' with G' is not seen because, in mechanical rheometry, the data are restricted to $\omega \approx 100$ rad/s.

WLM rheology at higher ω has been addressed in recent years,^{14–21} and a typical data set is shown in Figure 1b. The

sample consists of the cationic surfactant cetyltrimethylammonium bromide (CTAB, 350 mM) combined with sodium chlorate (NaClO_3 , 600 mM) in water. These data are from a paper by Oelschlaeger et al. and were obtained by superposing measurements from three techniques:¹⁷ rheometry (at low ω), oscillatory squeeze flow (OSF, higher ω), and diffusive wave spectroscopy (DWS, highest ω), all at 30 °C. We again note the terminal regime at low ω (where $G'' > G'$), and then the elastic regime at medium ω , where $G' = G_p$ exceeds G'' , while the latter goes through a minimum and an upturn. At higher ω , a second crossover of the moduli is seen, and this is the feature missing from Figure 1a. Overall, the sample exhibits two crossover frequencies: the first at $\omega_{c1} \approx 10$ rad/s marks the boundary of the terminal regime, while the second at $\omega_{c2} \approx 3 \times 10^4$ rad/s marks the boundary of the elastic regime. We can conclude that WLMs in water will exhibit two crossovers of their moduli that are widely separated by several decades of frequency, i.e., the ratio $\omega_{c2}/\omega_{c1} > 10$.³

Regarding the physical meaning of the third regime at $\omega > \omega_{c2}$, it can be termed the “breathing” regime.^{11,22} At these very short timescales, the rheology reflects the dynamics of individual chain segments in an intact network. The chain segments will relax only via bending or “breathing” motions (Rouse-Zimm modes).^{15,23} In this regime, both moduli are functions of ω , with $G'' > G'$ as in the terminal regime. The breathing regime has been well-studied for entangled polymer solutions and melts.^{11,23,24} For these systems, the time-temperature superposition (TTS) technique is used to access a wide range of ω . However, TTS cannot be used for WLMs because the WLM length changes with temperature.^{1,9,13} Thus, to cover all three regimes (terminal, elastic, breathing) for WLMs, a wide range of ω must be accessed at a *single temperature*, and this can be done only by resorting to advanced techniques like OSF and DWS, not by rheometry. Note that the ω -axis in Figure 1b spans from 10^{-2} to 10^6 rad/s, i.e., across eight decades of frequency.

For comparison, a typical plot of G' and G'' vs ω for WLMs in glycerol is shown in Figure 1c. The sample consists of EHAC (60 mM) combined with NaSal (60 mM), and the entire dataset is from rheometry at 25 °C. In this case, over an ω -range of just three decades (10^{-1} to 10^2 rad/s) we find all the three regimes noted in Figure 1b (terminal, elastic, and breathing). There are two crossovers of G' and G'' : at frequencies $\omega_{c1} \approx 1$ rad/s and $\omega_{c2} \approx 10$ rad/s. Thus, the elastic regime spans only one decade in ω , and in fact G' keeps increasing over this regime instead of reaching a plateau. Also, the transition to the breathing regime occurs at a frequency ω_{c2} that is 10^4 times lower than for the aqueous WLMs in Figure 1b, thereby allowing this regime to be accessed easily by rheometry. Clearly, the rheology of WLMs in glycerol is very different from that of aqueous WLMs. Incidentally, the lines through the data in Figure 1c are fits to a generalized Maxwell model that includes three modes,^{11,23} each with a different G_p and t_R . The values of these parameters for the three modes are shown in Figure S1 in the Supporting Information (SI).

Rheology of WLMs in Glycerol as a Function of Temperature. The data in Figure 1c are for a 60/60 EHAC/NaSal sample in glycerol at 25 °C. It is useful to examine the dynamic rheological data for the above sample as a function of temperature T . Data were collected on this sample from 10 to 50 °C in increments of 1 °C, and a subset of this data from 25 to 40 °C are shown in a single plot in Figure 2a. As T increases, the contour length L of the WLMs decreases exponentially,

and hence, the WLMs relax exponentially faster.^{6,13} In turn, the zero-shear viscosity of the WLM solutions also plummets.⁶ The shortening of the WLMs explains the broad trend in Figure 2a where both G' and G'' shift toward higher ω with increasing T . A second trend is that the terminal regime is more pronounced at higher T while the elastic and breathing regimes are more apparent at lower T . In the terminal regime, $G'' > G'$, with the slopes of G' and G'' being close to 2 and 1, respectively, as expected for typical WLMs and polymeric fluids.^{11,23} After the moduli cross at ω_{c1} , G' overtakes G'' in the elastic regime. Thereafter, the moduli cross again at ω_{c2} , and $G'' > G'$ in the breathing regime. From the crossover frequencies at each T , we calculate $t_{R1} = 1/\omega_{c1}$, which is the “long” relaxation time, and $t_{R2} = 1/\omega_{c2}$, which is the “short” relaxation time.

Data at specific temperatures are highlighted in Figure 2b–d, and these reflect different prototypical shapes (or patterns) for the G' and G'' curves. At 15 °C (Figure 2b), G' and G'' cross twice, similar to Figure 1c. Between the crossover points, the curves form a loop, and both the width (i.e., range of ω) and the area of this loop decrease with increasing T . This pattern persists between 15 and 30 °C. A new pattern arises at 31 °C (Figure 2c): in this case, the moduli cross thrice, with two of these occurring in the breathing regime. These unusual data are observed only from 31 to 33 °C. For $T \geq 34$ °C, G' and G'' cross just once, as exemplified by the data at 40 °C in Figure 2d. At this point, the loop between G' and G'' has vanished, and there appears to be a direct jump from the terminal to the breathing regime. The lack of an elastic regime at these higher T may imply that the WLMs have shortened appreciably by this point such that the chains are unable to form an entangled network.^{19,21} Also, note that the two moduli in the breathing regime in Figure 2d are very close to each other (nearly overlap) over a range of ω .

Parameters extracted from the dynamic spectra in Figure 2 are shown in Figure 3. The crossover frequencies ω_{c1} , ω_{c2} , and ω_{c3} are plotted vs T on a log-linear plot in Figure 3a. A linear relationship is found for both ω_{c1} and ω_{c2} over the range of T . This means that the corresponding relaxation times t_{R1} and t_{R2} decrease exponentially with T ,^{1,9} as further shown by the Arrhenius plots in SI Figure S2. Note that ω_{c2} does not exist above 33 °C and it is only in a small window near this temperature that ω_{c3} is measured. Incidentally, a third crossover is known to occur in the dynamic rheology of many polymer melts²³ as well as bottlebrush polymers²⁴ (in all those cases, TTS is required to access a wide range of ω). Another parameter of interest is the (pseudo) plateau modulus G_p . Although G' does not reach a true plateau, G_p can be estimated as the value of G' when the loss tangent $\tan \delta = G''/G'$ reaches a minimum. We find that G_p is nearly constant (between 13 and 16 Pa) from 10 to 33 °C, as shown in SI Figure S3. Beyond 33 °C, the elastic regime is absent and hence G_p is undefined.

Some implications of the above results are worth noting. It is known that G_p inversely correlates with the mesh size of the transient WLM network.^{11,21} Thus, the constancy of G_p means that the network mesh size is constant from 10 to 33 °C. Also, provided the WLMs are long enough to entangle, G_p will be independent of their contour length L .^{11,21} In other words, each WLM will be entangled many times with other WLMs. The distance along the micellar network between any two entanglement points is called the entanglement length L_e .^{1,21} A parameter that characterizes chain entanglement is the average

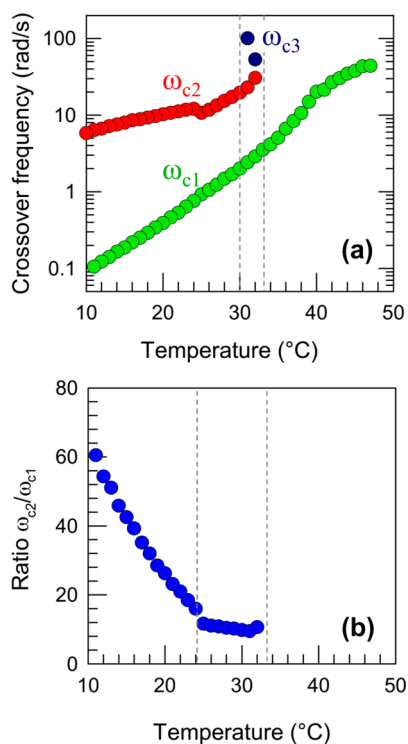


Figure 3. Parameters extracted from the temperature-dependent rheology of WLMs in glycerol. The parameters are from the data in Figure 2 for a sample of 60 mM EHAC + 60 mM NaSal in glycerol. (a) Crossover frequencies ω_{c1} , ω_{c2} , and ω_{c3} as functions of temperature. (b) Ratio of ω_{c2}/ω_{c1} as a function of temperature.

number of entanglements per WLM chain, $Z = L/L_e$. Recent studies have correlated Z with the ratio of ω_{c2}/ω_{c1} .^{19,21} We have computed the above ratio of frequencies and plotted it against T in Figure 3b. The results indicate a monotonic, linear decrease in this ratio—from 60 at 10 °C to 15 at 25 °C—and thereafter, the ratio remains constant until 33 °C. This suggests that the WLMs are long and highly entangled (high Z , i.e., $L \gg L_e$) at low T . Increasing T decreases L and thus decreases Z . Our analysis also reveals one important difference between

WLMs in glycerol and those in water. For WLMs in glycerol, the highest ratio of ω_{c1}/ω_{c2} is about 60. For WLMs in water, the ratio of ω_{c1}/ω_{c2} can be 10^3 or higher, indicating a much higher Z . From these results, we can infer that WLMs in glycerol are *much shorter* (and thus have far fewer entanglements per chain) compared to WLMs in water.

A common way to show the Maxwellian behavior of WLMs in water is by using the Cole–Cole plot, which is a linear plot of G'' vs G' .^{1–4} The Cole–Cole plot for a Maxwell fluid will be a perfect semicircle, with the diameter of the semicircle being the plateau modulus G_p . We had previously shown the Maxwellian rheology of WLMs in water in Figure 1a. The Cole–Cole plot of this data is shown in Figure 4a, and indeed it is close to a semicircle. For comparison, the data for WLMs in glycerol at 25 °C (from Figure 1c) are also shown in Figure 4a. In this case, the Cole–Cole plot deviates from the semicircular shape and extends as a near-straight line. Data for the glycerol sample at various temperatures are plotted in the Cole–Cole format in Figure 4b. As T is increased, the plots initially follow semicircular arcs (see inset), with the diameter of the arc being higher at higher T . However, the plots then deviate from the arc and extend as straight lines. These lines fan out from the initial region, and the slopes of the lines decrease with increasing T .

Rheology of WLMs in Glycerol as a Function of Salt.

In the previous section, we described the rheology of WLMs in glycerol as a function of temperature. Several other variables can be used to alter the rheology of these WLMs,⁶ including the concentration of the EHAC surfactant, the concentration of salt (NaSal), and the type of salt. Regardless of the variable studied, a range of samples exhibit the unusual rheology described above with two crossovers of G' and G'' . To illustrate this, we focus on the NaSal concentration and show how it affects the rheology at a single temperature of 25 °C (Figure 5). The EHAC concentration is fixed at 60 mM and only NaSal is varied. SI Figure S4 shows the zero-shear viscosity η_0 as a function of NaSal from steady-shear rheology for these samples; these data were presented in our earlier paper⁶ and are shown here for reference. The plot indicates an increase in η_0 with added salt until a maximum is reached at 48 mM NaSal. With further increases in salt content, η_0 drops and

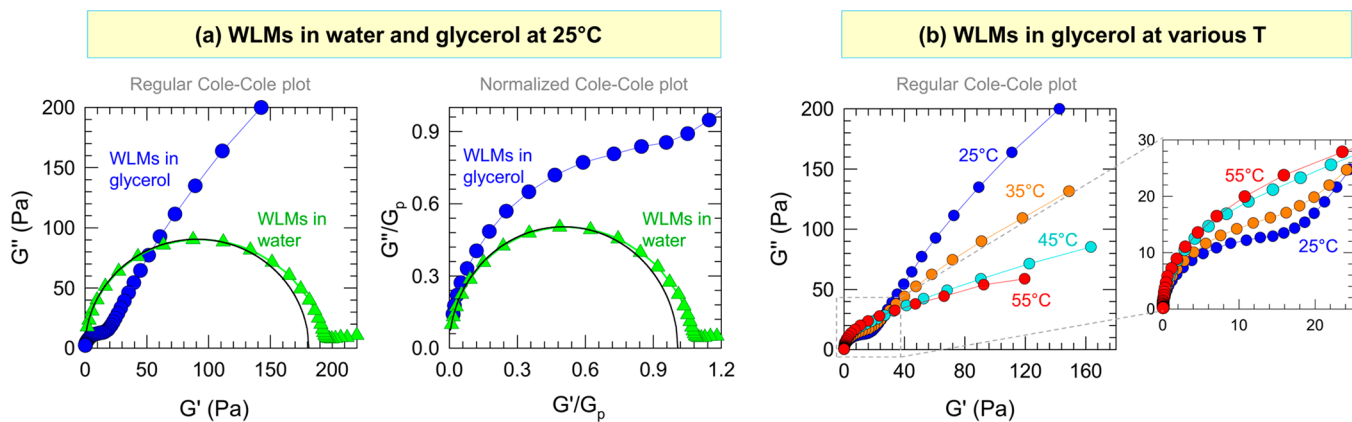


Figure 4. Cole–Cole plots for WLMs in water and glycerol. The regular Cole–Cole plot is one of G'' vs G' , with both axes on a linear scale. The normalized plot depicts the moduli scaled by the plateau modulus G_p . (a) Comparison via Cole–Cole plots at 25 °C of WLMs in water (data from Figure 1a) and WLMs in glycerol (data from Figure 1c). The aqueous sample is a Maxwell fluid, which yields a semicircle on the plots. The glycerol sample deviates from the semicircular arc and extends as a straight line. (b) Cole–Cole plots for WLMs in glycerol at various temperatures (data from Figure 2a). The plots fan out in a series of straight lines at higher moduli. The inset shows the initial portion of the graph, where the order of semicircular arcs is reversed.

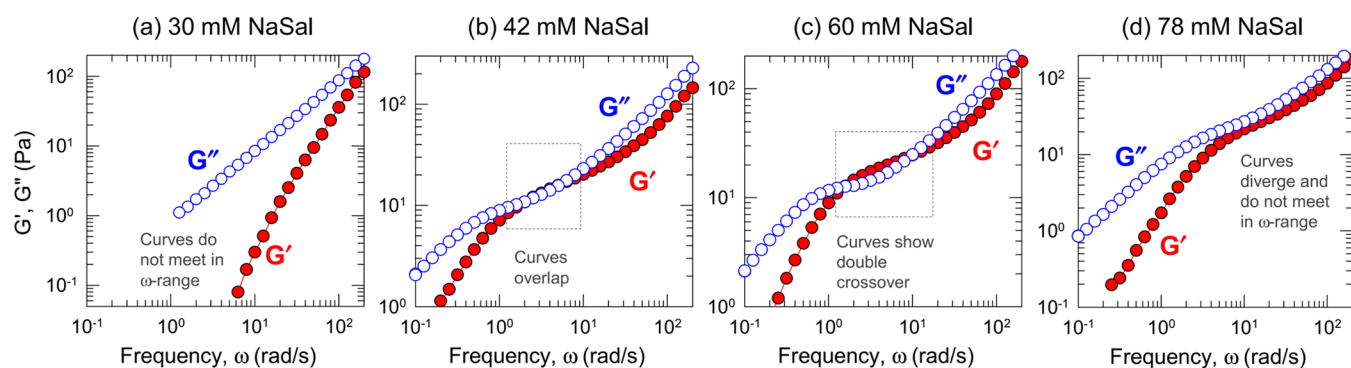


Figure 5. Dynamic rheology of WLMs in glycerol at various salt concentrations. In all cases, the elastic modulus G' and the viscous modulus G'' are plotted vs frequency ω . All experiments were done at 25 °C. The samples contain 60 mM EHAC and varying concentrations of salt (NaSal): (a) 30 mM; (b) 42 mM; (c) 60 mM; and (d) 78 mM.

reaches a plateau. Thus, WLM formation in glycerol is maximized when the salt and surfactant are at close to equimolar levels.

The dynamic rheology of selected samples (both to the left and to the right of the viscosity-maximum) are shown in Figures 5a–d. At low NaSal, as typified by the data for 30 mM NaSal in Figure 5a, the response is purely viscous, with only the terminal region ($G'' > G'$ at all ω) being observed in the data. As the NaSal is increased, the response becomes viscoelastic. For instance, at 42 mM NaSal (Figure 5b), G' and G'' overlap over an intermediate range of ω . At 60 mM NaSal, the double-crossovers of G' and G'' are observed (Figure 5c), which is the pattern discussed in detail previously. Above 60 mM NaSal, the loop area between G' and G'' decreases and eventually drops to zero; correspondingly, the viscosity η_0 also drops. For example, in Figure 5d for 78 mM NaSal, G' and G'' are separate curves that do not cross, indicating a loss of viscoelasticity. Note the similarity between the curves in Figure 5d and those in Figure 2d for a lower NaSal but a higher temperature.

Differences Between WLMs in Glycerol and Water.

We have demonstrated that WLMs in glycerol exhibit very different responses in dynamic rheology compared to WLMs in water. The differences can be summarized as follows:

- (1) WLMs in water are Maxwell fluids with a single t_{br} and this manifests as a semicircle on a Cole–Cole plot. WLMs in glycerol are *not* Maxwell fluids; rather they exhibit a spectrum of relaxation times and their response deviates sharply from a semicircle on a Cole–Cole plot.
- (2) WLMs in water exhibit a single crossover of G' and G'' (at ω_{c1}) in the ω -range accessible by rheometry. WLMs in glycerol exhibit **two crossovers** of G' and G'' (at ω_{c1} and ω_{c2}) in the ω -range accessible by rheometry. In a few cases, a third crossover (at ω_{c3}) is also seen.
- (3) WLMs in water exhibit a second crossover of G' and G'' at $\omega_{c2} \approx 10^4$ rad/s, above which is the “breathing regime”, corresponding to segmental motion of the chains. Data at such high ω can be recorded only by advanced techniques like OSF and DWS. The ratio of ω_{c2}/ω_{c1} is $>10^3$ for these WLMs. In contrast, for WLMs in glycerol, ω_{c2} occurs around 10 rad/s, i.e., the breathing regime is reached at much lower ω , and the **ratio of ω_{c2}/ω_{c1} is only ~ 10 .**

Why do these differences arise, and what does it tell us about WLMs in glycerol? To understand the origin of these differences, we need to discuss how glycerol differs from

water as a solvent. There are two factors in this regard: (a) glycerol is much more viscous than water; and (b) the propensity of surfactants to self-assemble into micelles is much lower in glycerol than in water. With regard to (b), self-assembly in water is driven by the hydrophobic effect,^{25–27} which is a strong interaction mainly due to the unique properties of water. In comparison, the driving force for self-assembly in glycerol is the “solvophobic effect”,^{7,8,27} which is much weaker. This is why there are no examples of WLMs in pure glycerol apart from our own previous study.⁶ Due to the weaker driving force for self-assembly in glycerol, **WLMs in glycerol are likely to be shorter**, i.e., have lower contour lengths L compared to WLMs in water. The shorter WLMs will also have fewer entanglements per chain (lower $Z = L/L_e$), which partly explains why the ratio of ω_{c2}/ω_{c1} is much lower in glycerol than in water.^{19,21}

We also hypothesize a second difference: that the WLMs in glycerol are much less dynamic, i.e., that they break and recombine much less frequently compared to WLMs in water. In other words, the breaking time t_{br} for WLMs in glycerol will be much greater than the t_{br} for WLMs in water. The reason for this difference is tied to the higher viscosity of glycerol. The viscosity of glycerol is substantially higher than that of water across the temperature range investigated in this work (see SI Figure S5). For instance, the ratio of their viscosities is about 1500 at 15 °C, and it drops to about 400 at 45 °C. For a WLM to break in glycerol, surfactant unimers will have to diffuse out of a micelle in unison or in close succession.^{26,27} However, the timescale for such diffusion will be quite long because the solvent is so viscous. Thus, while individual surfactants may temporarily leave the WLM, the micelle may still not break, or its t_{br} will be very high. If our hypothesis is correct, then WLMs in glycerol will never be in the fast breaking limit ($t_{br} \ll t_{rep}$), and this can explain why their rheology is never Maxwellian. The point then is that **WLMs in glycerol behave, not like micelles, but like polymers**—due to the “unbreakable” nature of the chains.

The third key aspect is regarding the **role of the viscous solvent toward the rheology** of the WLMs in glycerol.^{23,28} As noted earlier, when WLMs are in the breathing regime at high ω , the chains will undergo segmental motions. The timescales associated with these segmental motions will be dictated by a friction or drag coefficient, which will be proportional to the solvent viscosity.^{23,28} Thus, a 1000-fold increase in solvent viscosity will imply a comparable increase in the breathing timescales, which will, in turn, push the breathing regime to

1000-fold lower frequencies.^{19,21} The increase in friction coefficient will also have a comparable effect in pushing the terminal regime as well to lower frequencies.^{23,28} Taken together, we suggest that glycerol influences the rheology in two ways. On the one hand, because glycerol is highly viscous, the crossover at ω_{c2} will be pushed to lower frequencies, i.e., to ~ 10 rad/s. In addition, because glycerol is less polar than water, the WLMs formed in glycerol will be relatively short and weakly entangled. Thus, the ratio of ω_{c2}/ω_{c1} will be a low value ~ 10 . This implies that the first crossover at ω_{c1} will occur at a relatively high value of ~ 1 rad/s. Accordingly, both ω_{c1} and ω_{c2} fall within the ω -window accessible by rheometry. Note that if a sample only had short WLMs, but the solvent was of low-viscosity (like water), then we may only observe a single crossover (at ω_{c1}) of the moduli via rheometry.^{19,21} A viscous solvent may be necessary to observe the unusual double-crossover of G' and G'' within just a decade of ω .

CONCLUSIONS

We have demonstrated that the dynamic rheology of WLMs in glycerol is very different from that of WLMs in water. WLMs in glycerol are not Maxwell fluids; on the contrary, they exhibit an unusual double-crossover of G' and G'' (at ω_{c1} and ω_{c2}), with the entire set of data falling within the ω -window accessible by rheometry (10^{-2} to 10^2 rad/s). At frequencies above ω_{c2} , the rheology is dominated by the segmental motion of chains in the “breathing regime”—this regime has been rarely accessed for WLMs, although it is well-documented for polymer solutions and melts. We believe that glycerol, a solvent that is much more viscous than water, is responsible for pushing ω_{c2} to relatively low values around 10 rad/s; in comparison, ω_{c2} for WLMs in water is at least 1000-fold higher. Our rheological studies suggest that WLMs in glycerol are shorter and entangled only weakly compared to WLMs in water. This is consistent with the fact that self-assembly in glycerol occurs to a lesser extent than in water. In terms of their dynamics, we hypothesize that WLMs in glycerol are more similar to polymers—i.e., that the chains remain intact rather than breaking and re-forming frequently. If the breaking time t_{br} of these WLMs is comparable or higher than the chain reptation time t_{rep} , then it would explain why the samples do not behave like Maxwell fluids.

ASSOCIATED CONTENT

Supporting Information

The Supporting Information is available free of charge at <https://pubs.acs.org/doi/10.1021/acs.langmuir.0c00489>.

Additional rheological data and further analysis of the data in Figures S1–S5, as described in the text (PDF)

AUTHOR INFORMATION

Corresponding Author

Srinivasa R. Raghavan – Department of Chemical & Biomolecular Engineering, University of Maryland, College Park, Maryland 20742, United States; orcid.org/0000-0003-0710-9845; Email: sraghava@umd.edu

Authors

Niti R. Agrawal – Department of Chemical & Biomolecular Engineering, University of Maryland, College Park, Maryland 20742, United States

Xiu Yue – Department of Chemical & Biomolecular Engineering, University of Maryland, College Park, Maryland 20742, United States; Xinjiang Technical Institute of Physics & Chemistry, Chinese Academy of Sciences, Urumqi 830011, P. R. China; orcid.org/0000-0002-4112-9535

Complete contact information is available at:
<https://pubs.acs.org/doi/10.1021/acs.langmuir.0c00489>

Notes

The authors declare no competing financial interest.

ACKNOWLEDGMENTS

We acknowledge fruitful discussions about this work with Prof. Michael Rubinstein (Duke University), Prof. Ronald Larson (University of Michigan), Dr. Jack Douglas (NIST), Dr. Steve Hudson (NIST), and Dr. Paul Salipante (NIST).

REFERENCES

- (1) Cates, M. E.; Candau, S. J. Statics and dynamics of worm-like surfactant micelles. *J. Phys.: Condens. Matter* **1990**, *2*, 6869–6892.
- (2) Rehage, H.; Hoffmann, H. Viscoelastic surfactant solutions - Model systems for rheological research. *Mol. Phys.* **1991**, *74*, 933–973.
- (3) Dreiss, C. A. Wormlike micelles: where do we stand? Recent developments, linear rheology and scattering techniques. *Soft Matter* **2007**, *3*, 956–970.
- (4) *Wormlike Micelles: Advances in Systems, Characterisation and Applications*; Dreiss, C. A., Feng, Y. J., Eds.; RSC: Cambridge, 2017.
- (5) Wang, J.; Feng, Y.; Agrawal, N. R.; Raghavan, S. R. Wormlike micelles versus water-soluble polymers as rheology-modifiers: similarities and differences. *Phys. Chem. Chem. Phys.* **2017**, *19*, 24458–24466.
- (6) Agrawal, N. R.; Yue, X.; Feng, Y. J.; Raghavan, S. R. Wormlike micelles of a cationic surfactant in polar organic solvents: Extending surfactant self-assembly to new systems and subzero temperatures. *Langmuir* **2019**, *35*, 12782–12791.
- (7) Warnheim, T. Aggregation of surfactants in nonaqueous, polar solvents. *Curr. Opin. Colloid Interface Sci.* **1997**, *2*, 472–477.
- (8) Greaves, T. L.; Weerawardena, A.; Drummond, C. J. Nanostructure and amphiphile self-assembly in polar molecular solvents: amides and the “solvophobic effect”. *Phys. Chem. Chem. Phys.* **2011**, *13*, 9180–9186.
- (9) Raghavan, S. R.; Kaler, E. W. Highly viscoelastic wormlike micellar solutions formed by cationic surfactants with long unsaturated tails. *Langmuir* **2001**, *17*, 300–306.
- (10) Macosko, C. W. *Rheology: Principles, Measurements, and Applications*; Wiley-VCH: New York, 1994.
- (11) Larson, R. G. *The Structure and Rheology of Complex Fluids*; Oxford University Press, New York, 1999.
- (12) Cates, M. E. Reptation of living polymers - dynamics of entangled polymers in the presence of reversible chain-scission reactions. *Macromolecules* **1987**, *20*, 2289–2296.
- (13) Tung, S. H.; Huang, Y. E.; Raghavan, S. R. Contrasting effects of temperature on the rheology of normal and reverse wormlike micelles. *Langmuir* **2007**, *23*, 372–376.
- (14) Buchanan, M.; Atakhorrami, M.; Palierne, J. F.; MacKintosh, F. C.; Schmidt, C. F. High-frequency microrheology of wormlike micelles. *Phys. Rev. E* **2005**, *72*, No. 011504.
- (15) Willenbacher, N.; Oelschlaeger, C.; Schopferer, M.; Fischer, P.; Cardinaux, F.; Scheffold, F. Broad bandwidth optical and mechanical rheometry of wormlike micelle solutions. *Phys. Rev. Lett.* **2007**, *99*, No. 068302.
- (16) Oelschlaeger, C.; Schopferer, A.; Scheffold, F.; Willenbacher, N. Linear-to-branched micelles transition: A rheometry and Diffusing Wave Spectroscopy (DWS) study. *Langmuir* **2009**, *25*, 716–723.

- (17) Oelschlaeger, C.; Suwita, P.; Willenbacher, N. Effect of counterion binding efficiency on structure and dynamics of wormlike micelles. *Langmuir* **2010**, *26*, 7045–7053.
- (18) Zou, W. Z.; Larson, R. G. A mesoscopic simulation method for predicting the rheology of semi-dilute wormlike micellar solutions. *J. Rheol.* **2014**, *58*, 681–721.
- (19) Zou, W. Z.; Tang, X. M.; Weaver, M.; Koenig, P.; Larson, R. G. Determination of characteristic lengths and times for wormlike micelle solutions from rheology using a mesoscopic simulation method. *J. Rheol.* **2015**, *59*, 903–934.
- (20) Morishima, K.; Inoue, T. High frequency viscoelastic measurements using optical tweezers on wormlike micelles of nonionic and cationic surfactants in aqueous solutions. *J. Rheol.* **2016**, *60*, 1055–1067.
- (21) Zou, W. Z.; Tan, G.; Jiang, H. Q.; Vogtt, K.; Weaver, M.; Koenig, P.; Beaucage, G.; Larson, R. G. From well-entangled to partially-entangled wormlike micelles. *Soft Matter* **2019**, *15*, 642–655.
- (22) Granek, R.; Cates, M. E. Stress-relaxation in living polymers - results from a Poisson renewal model. *J. Chem. Phys.* **1992**, *96*, 4758–4767.
- (23) Rubinstein, M.; Colby, R. H. *Polymer Physics*; Oxford University Press, 2003.
- (24) Daniel, W. F. M.; Burdyska, J.; Vatankhah-Varnoosfaderani, M.; Matyjaszewski, K.; Paturej, J.; Rubinstein, M.; Dobrynin, A. V.; Sheiko, S. S. Solvent-free, supersoft and superelastic bottlebrush melts and networks. *Nat. Mater.* **2016**, *15*, 183–190.
- (25) Jonsson, B.; Lindman, B.; Holmberg, K.; Kronberg, B. *Surfactants and Polymers in Aqueous Solutions*; Wiley: New York, 1998.
- (26) Evans, D. F.; Wennerstrom, H. *The Colloidal Domain: Where Physics, Chemistry, Biology, and Technology Meet*; Wiley-VCH: New York, 2001.
- (27) Israelachvili, J. N. *Intermolecular and Surface Forces*, 3rd ed.; Academic Press: San Diego, 2011.
- (28) Larson, R. G.; Sridhar, T.; Leal, L. G.; McKinley, G. H.; Likhtman, A. E.; McLeish, T. C. B. Definitions of entanglement spacing and time constants in the tube model. *J. Rheol.* **2003**, *47*, 809–818.

Supporting Information for:

The Unusual Rheology of Wormlike Micelles in Glycerol: Comparable Timescales for Chain Reptation and Segmental Relaxation

Niti R. Agrawal¹, Xiu Yue^{1,2}, and Srinivasa R. Raghavan^{1*}

¹Department of Chemical & Biomolecular Engineering, University of Maryland, College Park, Maryland 20742, USA

²Xinjiang Technical Institute of Physics & Chemistry, Chinese Academy of Sciences, Urumqi 830011, China

*Corresponding author. Email: sraghava@umd.edu

- Fig S1: Dynamic rheology of wormlike micelles in glycerol fit using multi-mode Maxwell models.
- Fig S2: Arrhenius plot of the relaxation times as a function of temperature for wormlike micelles in glycerol.
- Fig S3: Plateau modulus as a function of temperature for wormlike micelles in glycerol.
- Fig S4: Effect of NaSal concentration on the zero-shear viscosity of EHAC samples in glycerol.
- Fig S5: Solvent viscosity ratio (glycerol/water)

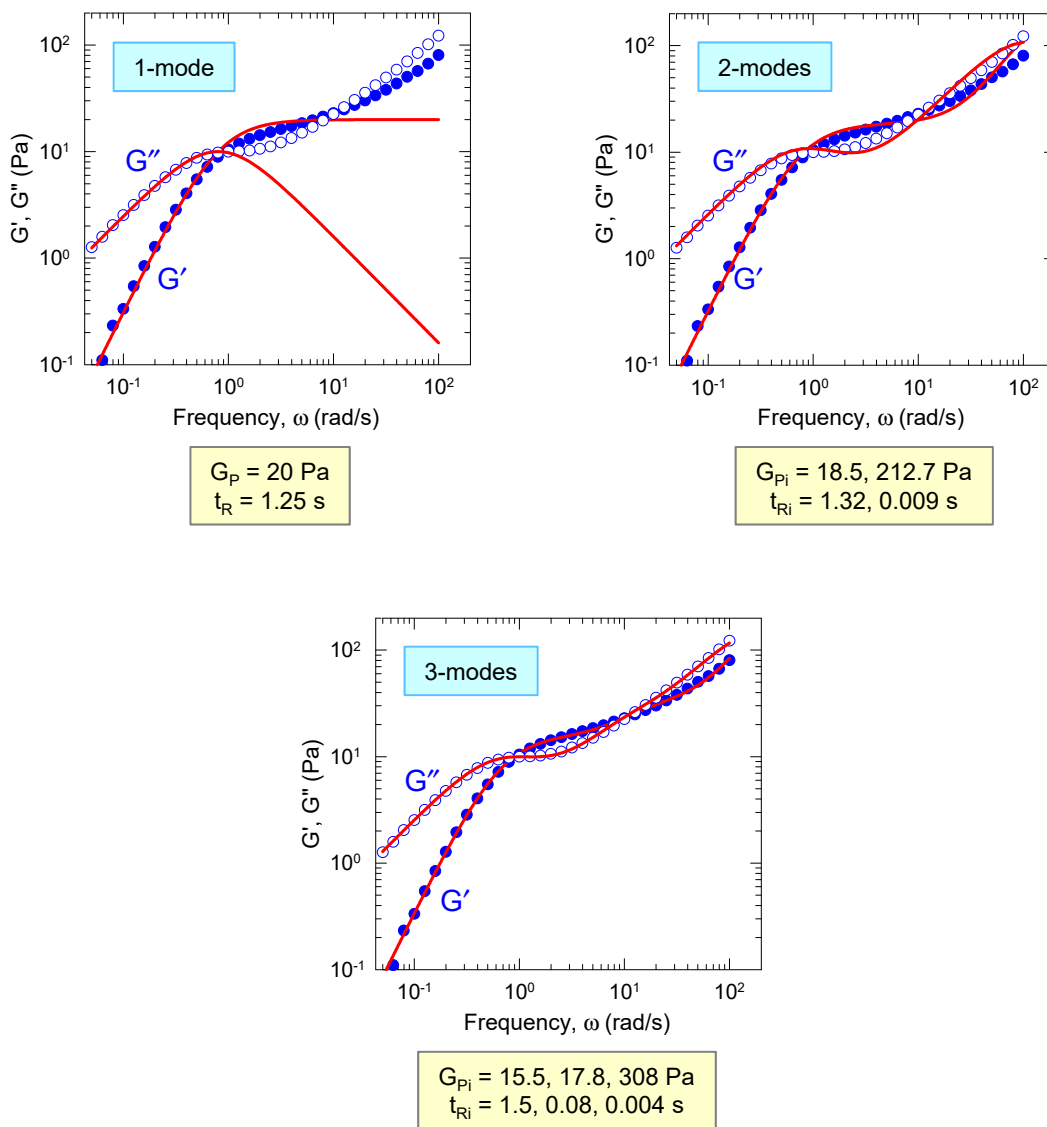


Figure S1. Dynamic rheology of wormlike micelles (WLMs) in glycerol fit using multi-mode Maxwell models. The data are those from Figure 1c and are for a sample of 60 mM EHAC + 60 mM NaSal at 25°C. The elastic modulus G' and the viscous modulus G'' are plotted vs. frequency ω . Fits to the data using 1-mode, 2-mode and 3-mode Maxwell models are shown in the three plots. The corresponding relaxation times (t_{Ri}) and plateau moduli (G_{pi}) are included. Note that a good fit over the entire ω -range is not obtained using just 1 or 2 modes.

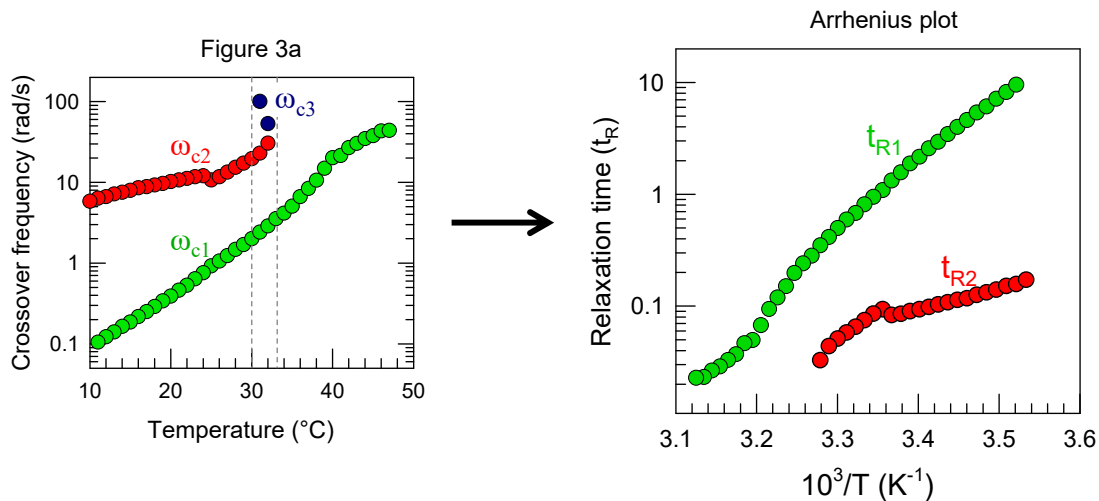


Figure S2. Arrhenius plot of the relaxation times as a function of temperature for wormlike micelles in glycerol. From the data in Figure 2 for a sample of 60 mM EHAC + 60 mM NaSal in glycerol, the crossover frequencies ω_{c1} and ω_{c2} were extracted and plotted vs. temperature on a log-linear plot in Figure 3a (reproduced above on the left). These data are converted into an Arrhenius plot on the right. The first (long) relaxation time $t_{R1} = 1/\omega_{c1}$ and the second (short) relaxation time $t_{R2} = 1/\omega_{c2}$ are plotted here vs. $1/T$ where T is the absolute temperature.

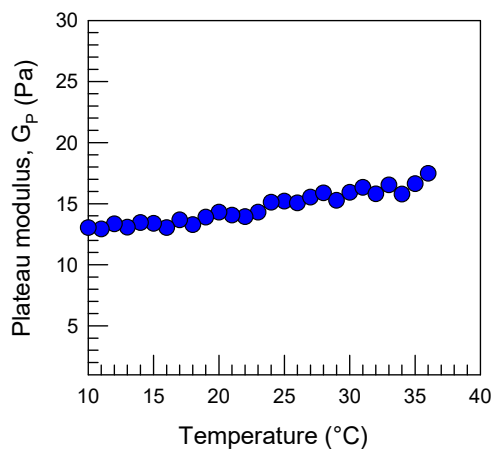


Figure S3. Plateau modulus G_p as a function of temperature for wormlike micelles in glycerol. From the data in Figure 2 for a sample of 60 mM EHAC + 60 mM NaSal in glycerol over a range of temperatures, G_p is estimated at each temperature as the value of G' when the loss tangent $\tan \delta = G''/G'$ reaches a minimum. The plot shows that G_p is relatively constant as a function of temperature.

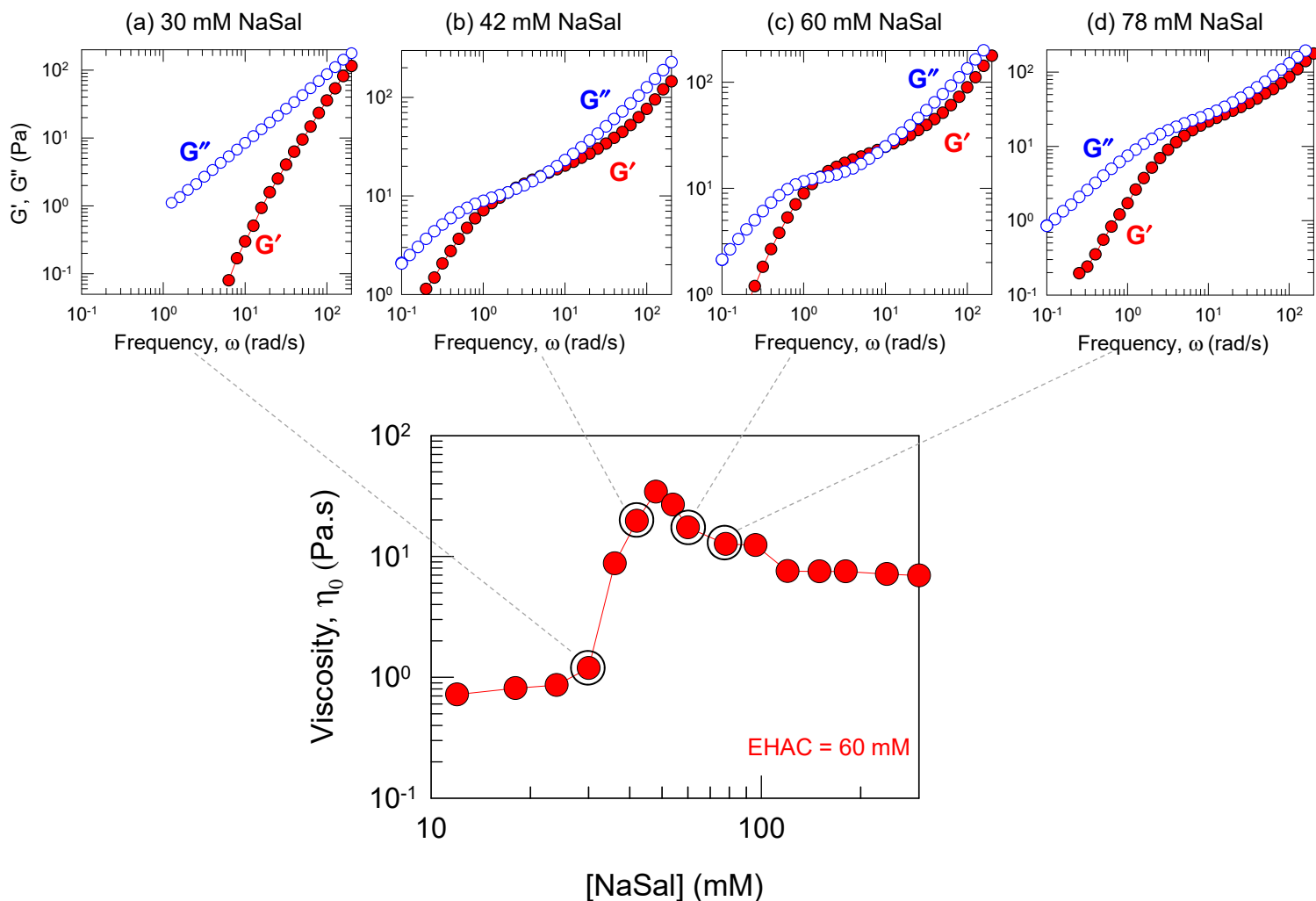


Figure S4. Effect of NaSal concentration on the zero-shear viscosity η_0 of EHAC samples in glycerol. Samples with varying NaSal (with EHAC constant at 60 mM) were characterized by steady-shear rheology at 25°C to obtain their respective η_0 values. This plot is a subset of the data shown in Ref. 6, and it reveals a maximum in η_0 around 48 mM NaSal. The plots from dynamic rheology in Figure 5 of the paper are reproduced above; these correspond to 30, 42, 60 and 78 mM NaSal. The selected samples, which are highlighted with circles on the viscosity plot, fall both to the left and the right of the viscosity maximum.

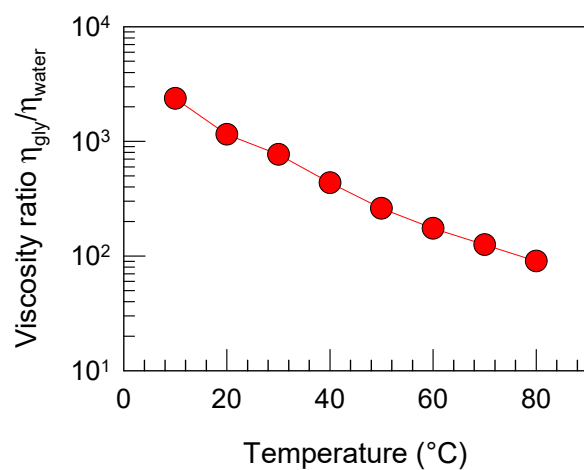


Figure S5. Solvent viscosity ratio (glycerol/water) at different temperatures. The ratio of the viscosities of glycerol and water (η_{gly}/η_{water}) is plotted over temperatures from 10 to 80°C. With increasing temperature, the ratio reduces significantly: from 2366 at 10°C to 90 at 80°C. Over the temperature range studied in Figure 2 (15 to 45°C), the ratio drops from ~1500 to ~400. Data for this plot were obtained from <https://wiki.anton-paar.com/us-en/water> and from Segur and Obertar, *Ind. Eng. Chem.* 1951, 43, 2117.